Available online at www.sciencedirect.com

ScienceDirect

Advances in Space Research 54 (2014) 59–71

ADVANCES IN SPACE RESEARCH (a COSPAR publication)

www.elsevier.com/locate/asr

Uncertainties and effects on geocenter motion estimates from global GPS observations

Xinggang Zhang [a,b], Shuanggen Jin [a,*]

[a] Shanghai Astronomical Observatory, Chinese Academy of Sciences, Shanghai 200030, China
[b] University of Chinese Academy of Sciences, Beijing 100049, China

Received 15 October 2013; received in revised form 18 March 2014; accepted 20 March 2014
Available online 30 March 2014

Abstract

Global positioning system (GPS) observations can be used to estimate the geocenter motion, but are subjected to large uncertainties and effects due to uneven distribution of GPS stations and high-degree aliasing errors. In this paper, uncertainties and effects on geocenter motion estimates from global GPS observations are investigated and assessed with different truncated degrees and selected GPS network distributions based on different plate motion models, including *NUVEL-1A*, *MORVEL56* and *ITRF08*. Results show that the selected GPS stations have no big effects on geocenter motion estimates based on different plate motion models, while large uncertainties are found at annual and semi-annual components when using different truncated degrees. Correlations of geocenter motion estimates from selected GPS networks with GRACE and SLR are better with truncated degree 3, and higher truncated degrees will degrade geocenter estimates. Smaller RMS also shows better results with the truncated degree 3 and the *NUVEL1A* has the worse results because more GPS sites are eliminated. For annual signal with truncated degree 3, four GPS strategies can reduce annual amplitudes by about 29.2% in *X*, 5.6% in *Y*, and 27.9% in *Z* with respect to truncated degree 1. Annual phases of all GPS solutions from *MORVEL56* and *ITRF08* are almost close to the GRACE solution with truncated degrees from 3 to 10, while the semi-annual signals are relatively weaker for all cases.

Keywords: Geocenter motion; Surface loading; GPS; GRACE; SLR

1. Introduction

The total mass of the whole Earth system consists of the solid Earth and the fluid envelope, such as the oceans, atmosphere and continental water (Jin et al., 2012, 2013). The transfer and redistributions of surface fluids can cause the surface loading deformation, geocenter motion (Swenson et al., 2008) and the Earth rotation variations (Jin et al., 2010, 2011). Currently, there are three types of geocenter definitions: center of the whole Earth (CM), center of solid Earth (CE), and center of figure (CF), which do not coincide with each other. The motion between CF and CM or between CE and CM are commonly called geocenter motion (Dong et al., 2003; Tregoning and van Dam, 2005; Wu et al., 2002). Here the geocenter motion is referred as CF relative to CM.

Geocenter motion was normally determined by tracking satellites orbiting around CM from stations located on Earth's surface, e.g., Satellite Laser Ranging (SLR) (Cheng et al., 2013). The other is inversed from the degree-1 deformation with a set of globally distributed geodetic observations based on the theoretical modeling of the Earth's elastic response to the loading stations (Lavallee et al., 2006; Wu et al., 2012). Blewitt et al. (2001) used 5 years

* Corresponding author. Tel.: +86 21 34775292; fax: +86 21 64384618.
E-mail addresses: sgjin@shao.ac.cn, sg.jin@yahoo.com (S. Jin).

http://dx.doi.org/10.1016/j.asr.2014.03.021
0273-1177/

of IGS GPS data at 66 stations to initially inverse degree-1 surface mass loading coefficients and corresponding geocenter motion with ignoring higher degrees. Wu et al. (2002) found that higher-degree terms would alias into degree-1 load coefficients since realistic network was not an even distribution. Later due to the lack of observations over the oceans, ocean bottom pressure (OBP) and GRACE data were combined to estimate the geocenter motion (e.g., Swenson et al., 2008).

The geocenter motion estimate from degree-1 loading inversion highly depends on the number and the distribution of GPS stations and suffers from aliasing errors of higher truncated degrees. Recently more and longer global GPS observations are available from January 2003 to 2013, which allow us to assess uncertainties and effects on geocenter motion estimates from global GPS observations. In this paper, the uncertainties and effects on geocenter motion estimates from global GPS observations are investigated with different GPS networks distribution and truncated degrees. Four strategies are designed to select GPS sites. One is using all GPS sites without removing deformed sites and the other three GPS networks are selected based on three plate motion models. Furthermore, annual and semi-annual geocenter variations and effects are studied with different truncated degrees, which are compared with SLR and GRACE plus OBP (hereafter called GRACE) (Swenson et al., 2008).

2. Surface loading theory

The Earth is usually assumed spherically symmetric, radially layered, elastic and statically loaded by a thin shell, including the atmosphere, oceans, and the continental water (Farrell, 1972). The large-scale surface mass redistribution within the Earth system mainly locates in the surface layer, which can be described by the surface density anomaly at a position (λ, θ) as (Wahr et al., 1998):

$$\Delta\sigma(\lambda,\theta,t) = a\rho_S \sum_{n=0}^{\infty}\sum_{m=0}^{n} \bar{P}_{nm}(\cos\theta)(\Delta C^{\sigma}_{nm}(t)\cos(m\lambda) + \Delta S^{\sigma}_{nm}(t)\sin(m\lambda)) \quad (1)$$

where a is Earth's mean radius, ρ_S seawater density, $\bar{P}_{nm}$ are the fully normalized associated Legendre polynomials, and $(\Delta C^{\sigma}_{nm}(t), \Delta S^{\sigma}_{nm}(t))$ are the time-varying spherical harmonic coefficients of the surface density anomaly.

The Earth surface mass loading can cause relative elastic displacements, which can be expressed as a spherical harmonic expansion according to the Love Number theory (Blewitt and Clarke, 2003):

$$\begin{aligned}
\Delta H(\lambda,\theta,t) &= \sum_{n=1}^{\infty}\sum_{m=0}^{n} h'_n \frac{3\rho_S}{(2n+1)\rho_E}\bar{P}_{nm}(\cos\theta)(\Delta C^{\sigma}_{nm}(t)\cos m\lambda + \Delta S^{\sigma}_{nm}(t)\sin m\lambda)\\
\Delta E(\lambda,\theta,t) &= \sum_{n=1}^{\infty}\sum_{m=0}^{n} l'_n \frac{3\rho_S}{(2n+1)\rho_E} m\bar{P}_{nm}(\cos\theta)(-\Delta C^{\sigma}_{nm}(t)\sin m\lambda + \Delta S^{\sigma}_{nm}(t)\cos m\lambda)\\
\Delta N(\lambda,\theta,t) &= \sum_{n=1}^{\infty}\sum_{m=0}^{n} l'_n \frac{3\rho_S}{(2n+1)\rho_E} \frac{\partial\bar{P}_{nm}(\cos\theta)}{\partial\theta}(\Delta C^{\sigma}_{nm}(t)\cos m\lambda + \Delta S^{\sigma}_{nm}(t)\sin m\lambda)
\end{aligned} \quad (2)$$

where ρ_S and ρ_E are mean density of the seawater (1025 kg m^{-3}) and the Earth (5517 kg m^{-3}), and h'_n and l'_n are load love numbers. The love numbers are used in the center of figure (CF) frame from Blewitt (2003):

$$\begin{aligned}
[l'_1]_{CF} &= 0.134\\
[h'_1]_{CF} &= -0.268
\end{aligned} \quad (3)$$

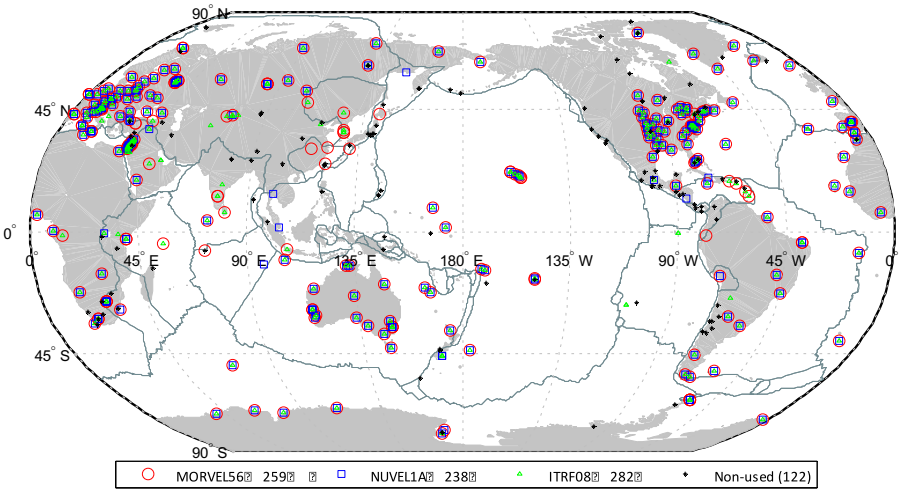

Fig. 1. Selected GPS networks distributions in this study. (For interpretation of the references to color in this figure legend, the reader is referred to the web version of this article.)

The degree-1 loading deformations are related to geocenter motion in terms of load moment components (Blewitt et al., 2001; Blewitt, 2003):

$$X = \frac{1}{M_\oplus} m_x = \frac{1}{M_\oplus} \frac{4\pi a^4 \rho_S}{3} \Delta C_{11}^\sigma$$
$$Y = \frac{1}{M_\oplus} m_y = \frac{1}{M_\oplus} \frac{4\pi a^4 \rho_S}{3} \Delta S_{11}^\sigma \quad (4)$$
$$Z = \frac{1}{M_\oplus} m_z = \frac{1}{M_\oplus} \frac{4\pi a^4 \rho_S}{3} \Delta C_{10}^\sigma$$

where $M_\oplus$ is mass of the Earth system and (m_x, m_y, m_z) are the loading vector.

3. GPS observations and selections

3.1. Global GPS observations

With the development of a wider and denser continuous GPS network, it can monitor geometrical changes of the Earth. The non-mass displacements, such as earthquake and antenna change, are removed from GPS time series. Furthermore, relatively stable stations are selected based on rigid plate motion models, which are located on stable plate and far from plate boundaries. Here we use global GPS daily time series provided at SOPAC (available at ftp://garner.ucsd.edu/pub/timeseries/) with removing the

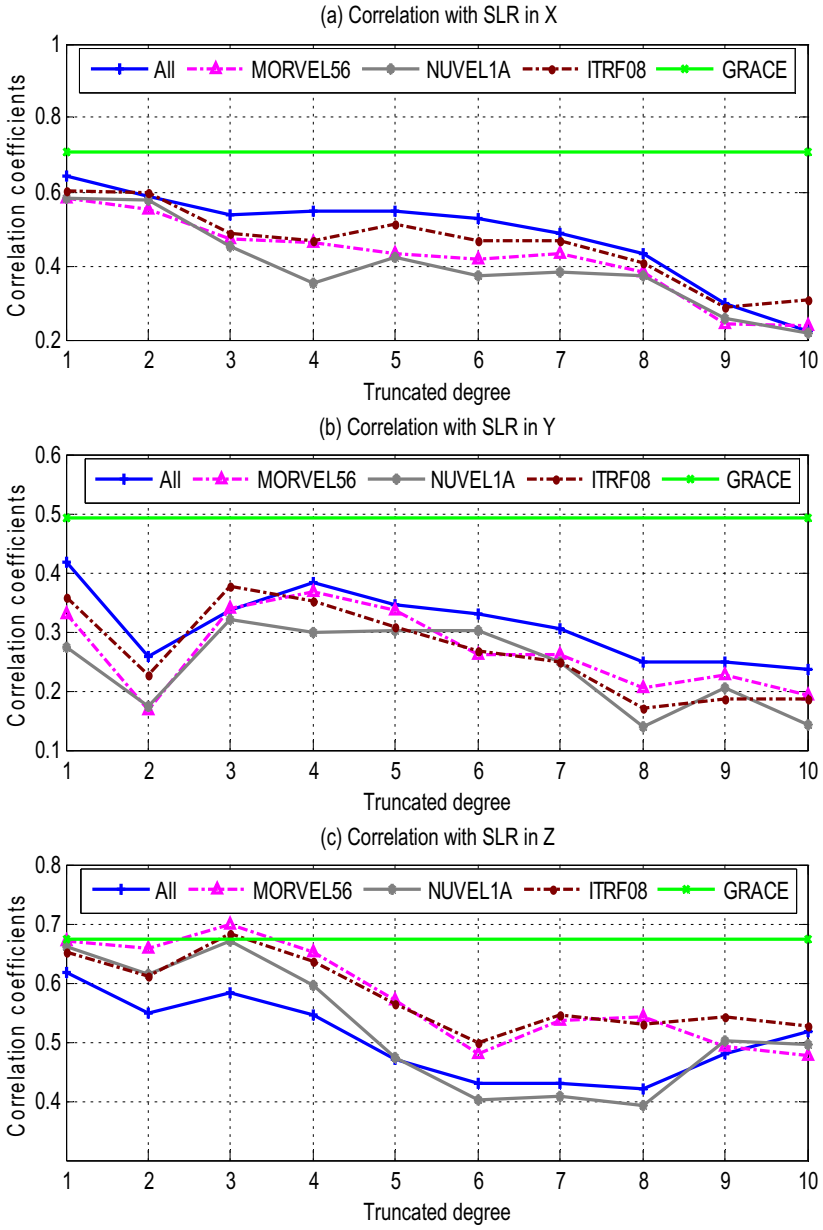

Fig. 2. Geocenter correlation of GPS and GRACE estimates with SLR. "All" means that all GPS sites are used without removing the deformed GPS sites, "MORVEL56" shows that the selected rigid GPS sites are based on the MOREVEL56 plate motion model, "NUVEL1A" means that the selected rigid GPS sites are based on the NUVEL1A plate motion model and "ITRF08" denotes that the selected rigid GPS sites are based on the ITRF08 plate motion model.

linear trend, outlier and mean value. In addition, some GPS observations with transient non-loading deformation are also removed.

3.2. GPS stations selection

Plate motion models describe the rigid plate motion. The rigid motion of each GPS site can be estimated as the following:

$$v_i = \Omega_p \times R_i \tag{5}$$

where v_i is the motion velocity, Ω_p is the angular velocity of the plate motion and R_i is the position vector. Three main plate models are used: *MORVEL56* (DeMets et al., 2010), *NUVEL1A* (DeMets et al., 1994; Jin and Zhu, 2004) and *ITRF08-PMM* (Altamimi et al., 2012) estimated from ITRF2008 GPS solutions.

The mean sigma of all GPS fitted velocities errors is 1.7 mm/y. GPS stations with deformation residuals between the observed minus estimated velocity of larger than three times of one sigma (i.e., 5.1 mm) are removed. Fig. 1 shows the selected GPS networks based on different plate motion models: 259 sites by *MORVEL56* (red circle), 238 by *NUVEL1A* (blue square), 282 by *ITRF08* (green triangle), and 122 unselected sites (black star) that are located nearby plate boundaries. In addition, another case of all GPS sites (*All*) is also tested without removing the deformed GPS sites.

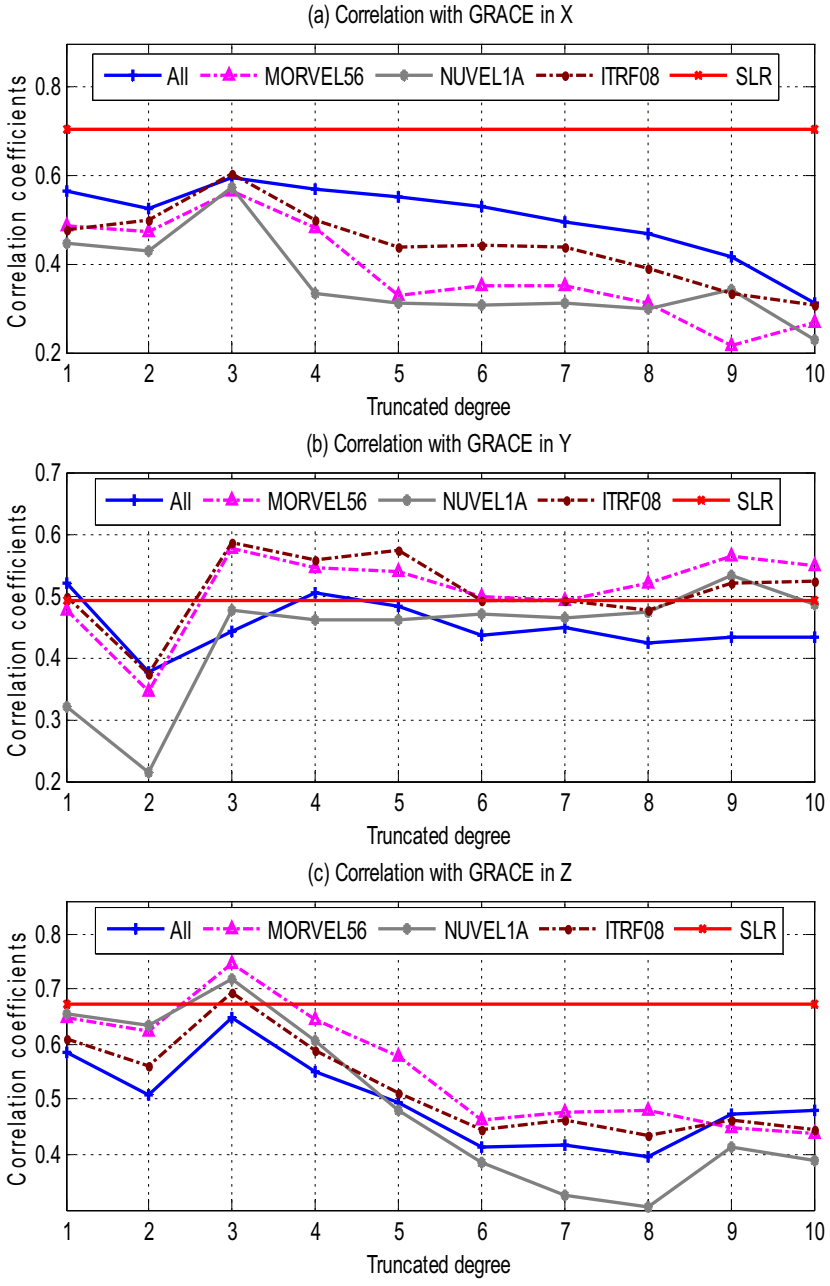

Fig. 3. Geocenter correlation of GPS and SLR estimates with GRACE. The symbols meanings are same as Fig. 2.

4. Estimation of geocenter motion

Theoretically, if GPS site distributions were globally homogenous, higher degree terms would not affect estimate of geocenter motion based on orthogonality of spherical harmonic functions over the entire Earth's surface. In practice, although hundreds of GPS stations are employed, no or less data are available around the polar and oceans areas, so geocenter motion could be contaminated by aliasing errors of higher degrees. In order to investigate effects of aliasing errors on the inversion of geocenter motion, the spherical harmonic load-induced geometrical displacements are truncated with degrees from 1 to 10, respectively.

The linear models of estimating unknown parameters are given by the matrix equation with a set of GPS station displacements:

$$Ax = b + \varepsilon \quad E(\varepsilon) = 0, \quad D(\varepsilon) = \sigma_0^2 P^{-1} \tag{6}$$

where b is the GPS displacements in the east, north and vertical, A is the design matrix with weight matrix P (dimension is $n \times m$, and m is number of unknown parameters), $x = [C_{10}^{\sigma}, C_{11}^{\sigma}, S_{11}^{\sigma}, \ldots, C_{NN}^{\sigma}, S_{NN}^{\sigma}]$ are the unknown parameters with truncation degree N and ε is the residual. The weighted least squares solutions is

$$\hat{x} = (A^T PA)^{-1} A^T Pb, \quad \hat{\sigma}_0^2 = \frac{V^T PV}{n - m} \tag{7}$$

where $V = A\hat{x} - b$ and $\hat{x}$ is the least-squares estimation of unknown vector x. After the coefficients are estimated, the geocenter coordinates (X, Y, Z) can be obtained from degree-1 coefficients based on the Eq. (4).

5. Results and discussion

5.1. Geocenter motion

The geocenter motions are estimated using the selected GPS networks with different truncated degrees from January 2003 to 2013. The correlations of GPS estimated results with SLR are shown in Fig. 2. The "All" means that all

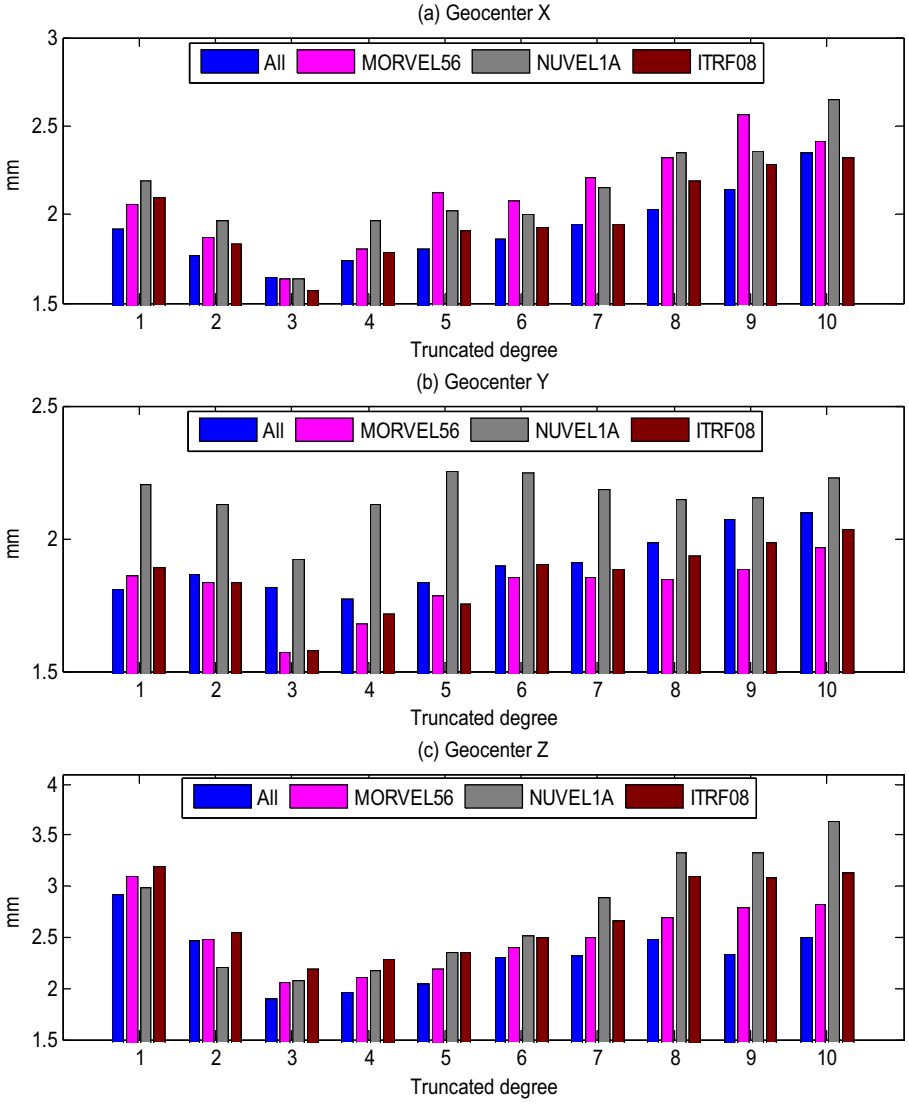

Fig. 4. RMS of GPS geocenter estimate with respective to GRACE. The symbols meanings are same as Fig. 2.

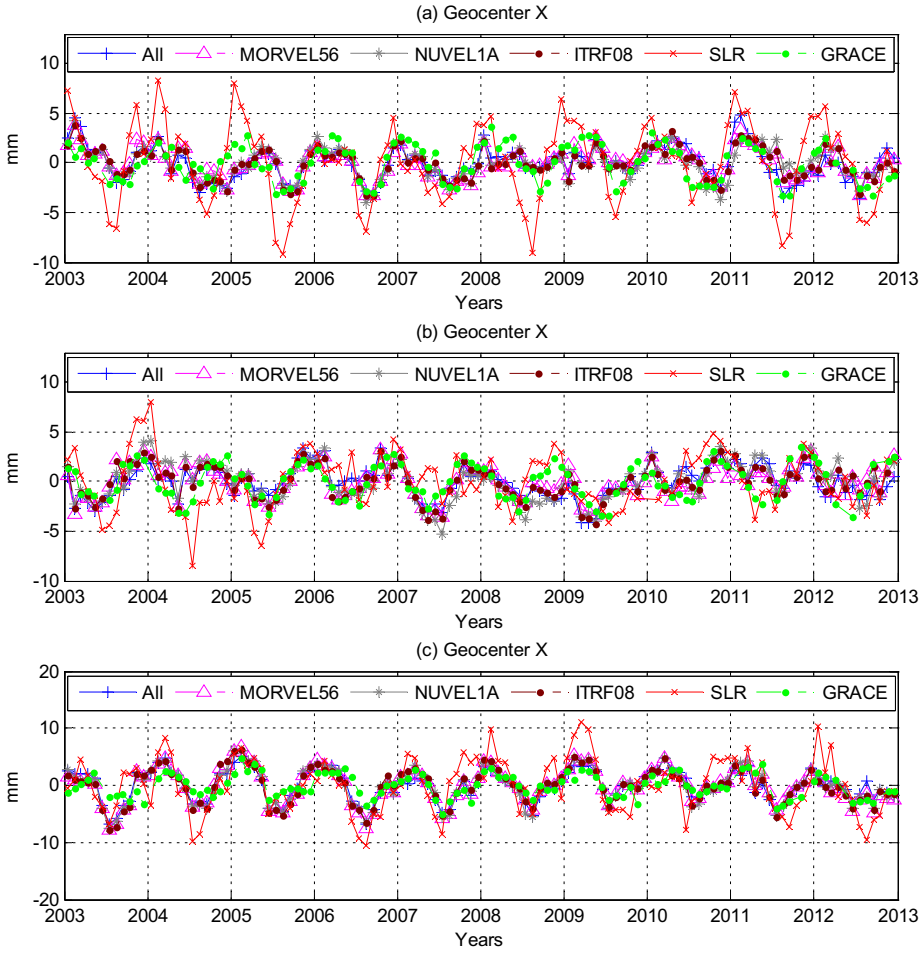

Fig. 5. The detrended time series of monthly geocenter motion estimates with truncated degree 3 (CF w.r.t. CM). The symbols meanings are same as Fig. 2.

Table 1
Annual amplitudes and phases of geocenter motion from different solutions with truncated degree 3. "All" means that all GPS sites are used, "MORVEL56" shows that the selected rigid GPS sites are based on the MOREVEL56 plate motion model, "NUVEL1A" means that the selected rigid GPS sites are based on the NUVEL1A plate motion model and "ITRF08" denotes that the selected rigid GPS sites are based on the ITRF08 plate motion model.

Strategies	X	σ_X	Y	σ_Y	Z	σ_Z
	Annual amplitude (mm)					
All	1.49	0.17	1.03	0.19	3.10	0.19
MORVEL56	1.25	0.16	1.44	0.16	3.47	0.23
NUVEL1A	1.46	0.16	1.63	0.21	3.60	0.20
ITRF08	1.42	0.15	1.55	0.17	3.52	0.21
SLR	4.37	0.29	2.26	0.30	4.54	0.42
GRACE	2.26	0.12	2.38	0.09	2.24	0.16
	Annual phase (°)					
All	64.66	6.57	−35.92	10.46	43.09	3.56
MORVEL56	71.22	7.12	−35.27	6.49	41.97	3.74
NUVEL1A	77.29	6.16	−12.29	7.38	42.31	3.20
ITRF08	76.96	5.95	−34.79	6.45	36.99	3.48
SLR	35.12	3.82	−23.54	7.44	39.74	5.24
GRACE	59.86	3.16	−39.70	2.15	69.13	4.26

GPS sites are used without removing the deformed GPS sites, "MORVEL56" means that the selected rigid GPS sites are based on the MOREVEL56 plate motion model, "NUVEL1A" denotes that the selected rigid GPS sites are based on the NUVEL1A plate motion model and "ITRF08" means that the selected rigid GPS sites are based

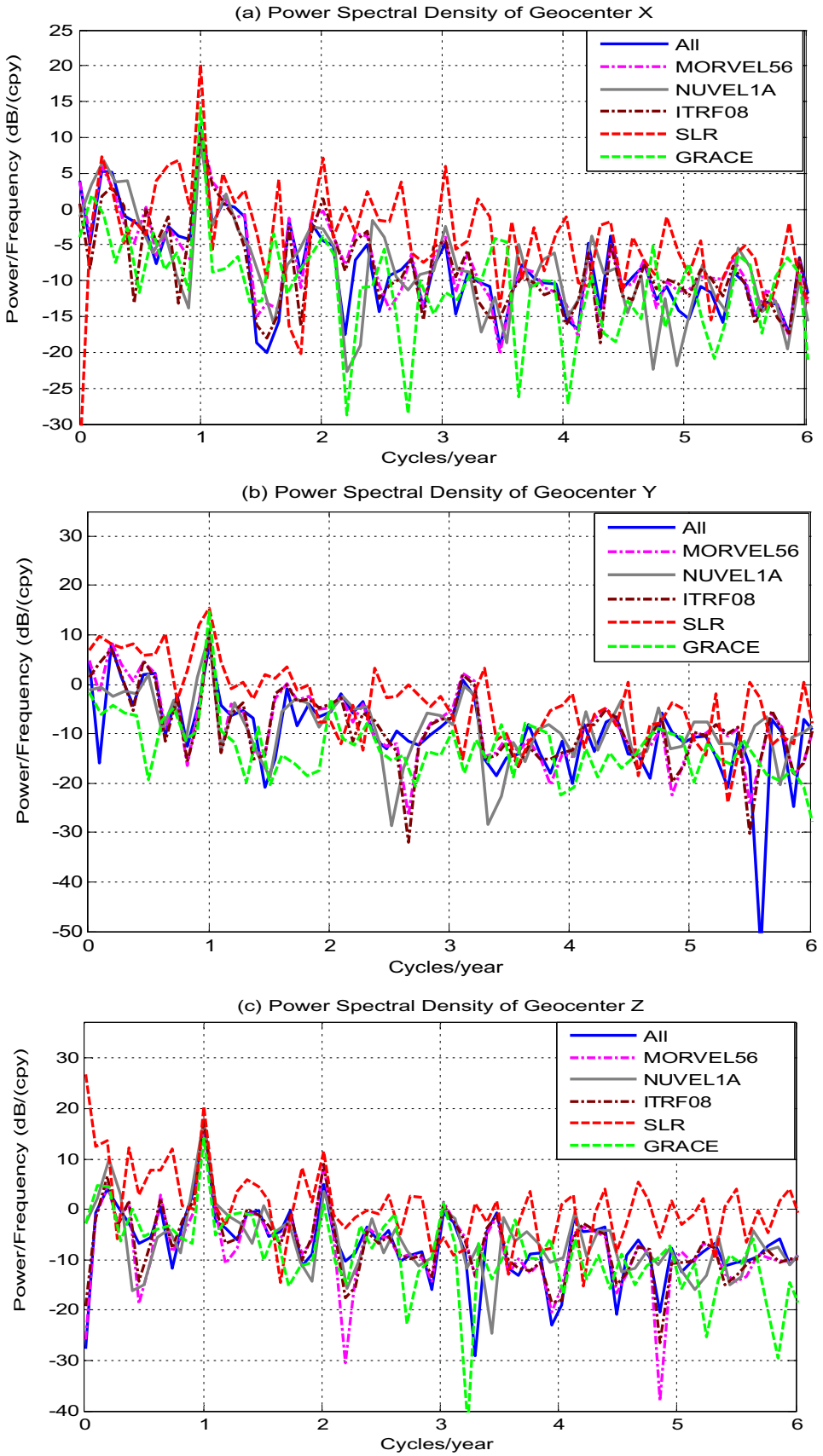

Fig. 6. Power spectral density of geocenter motions (X, Y and Z) from GPS observations with truncated degree 3. The symbols meanings are same as Fig. 2. The red line is the SLR estimate and the green line is GRACE solutions. (For interpretation of the references to color in this figure legend, the reader is referred to the web version of this article.)

Table 2
Semi-annual amplitudes and phases of geocenter motion from different solutions with truncated degree 3. The symbols meanings are same as Table 1.

Strategies	X	σ_X	Y	σ_Y	Z	σ_Z
	Semi-annual amplitude (mm)					
All	0.26	0.17	0.17	0.19	0.72	0.19
MORVEL56	0.34	0.16	0.26	0.16	0.70	0.23
NUVEL1A	0.32	0.16	0.23	0.21	0.81	0.20
ITRF08	0.39	0.15	0.14	0.17	0.71	0.21
SLR	1.06	0.29	0.29	0.29	1.69	0.42
GRACE	0.28	0.12	0.30	0.09	0.54	0.17
	Semi-annual phase (°)					
All	−19.52	38.22	−1.90	62.79	−146.91	15.36
MORVEL56	−26.38	26.50	42.66	36.30	−148.52	18.46
NUVEL1A	−4.05	28.32	−62.55	51.89	−146.26	14.30
ITRF08	−26.06	21.60	13.50	71.11	−137.13	17.30
SLR	−66.34	15.75	−48.99	59.18	−167.62	14.04
GRACE	−29.03	24.89	−178.35	17.03	−159.74	17.34

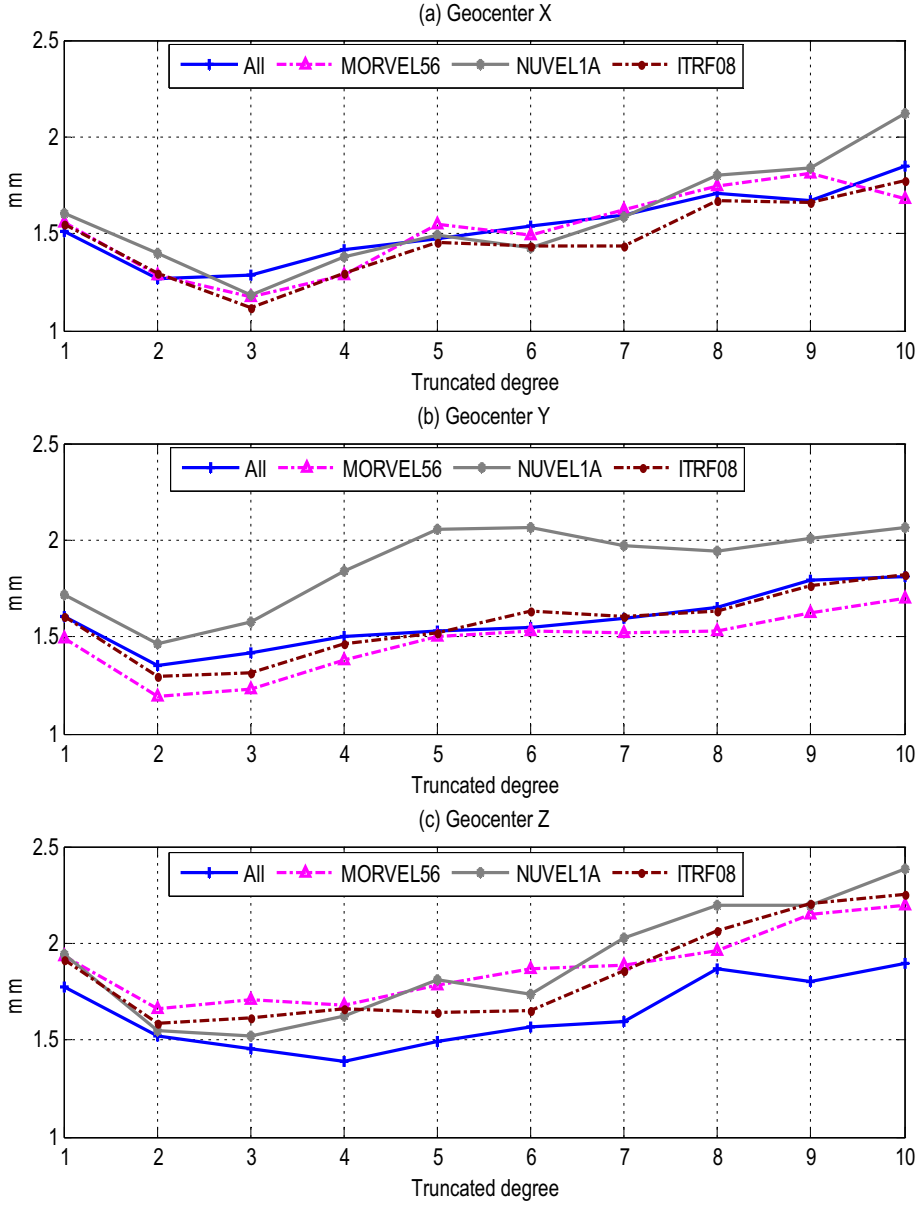

Fig. 7. RMS of residuals in geocenter motions (X, Y and Z) with different trancated degrees. The symbols meanings are same as Fig. 2.

on the ITRF08 plate motion model. Correlations are less than 0.5 in Y and worse than that in X and Z for all GPS strategies. With increasing truncated degrees, correlations of all GPS estimates with SLR in X decrease gradually, which is different from that in Y and Z. The results from GPS observations with truncated degree 3 are nearly better. Furthermore, most correlations from GPS estimates are lower than GRACE solutions, while GRACE results are closer to SLR solutions.

Fig. 3 shows the correlation of GPS results with GRACE. Correlations of GPS results with GRACE are higher. In particular Y direction, correlations of *MORVEL56* and *ITRF08* with GRACE are significant higher with over 0.5 with truncated degrees 3, 4 and 5. Furthermore, all correlations have minimum values with truncated degree 2 for each GPS strategy and maximum correlations are found with truncated degree 3 in each component for both *MORVEL56* and *ITRF08*. While the *NUVEL1A* performs worse in X and Y and good in Z with truncated degrees from 1 to 5.

In addition, correlations of geocenter motion estimated from GPS with SLR and GRACE are higher and RMSs of residuals are smaller in three components with truncated degree 3 (Fig. 4), indicating that good results with truncated degree 3 are obtained from GPS observations. Fig. 5 shows the detrended monthly geocenter motion time series with truncated degree 3 from January 2003 to 2013. There is almost no difference in GPS estimates between different strategies, which agree well with GRACE solutions in all three components. However, SLR amplitude is apparently larger than GPS and GRACE in X direction (also see Table 1). Fig. 6 shows the power spectral density of geocenter estimates from GPS. All estimates including SLR and GRACE present a clear annual period at the 1-cpy (cycle per year) frequency in three components, while semi-annual signal is relatively weak and does not agree

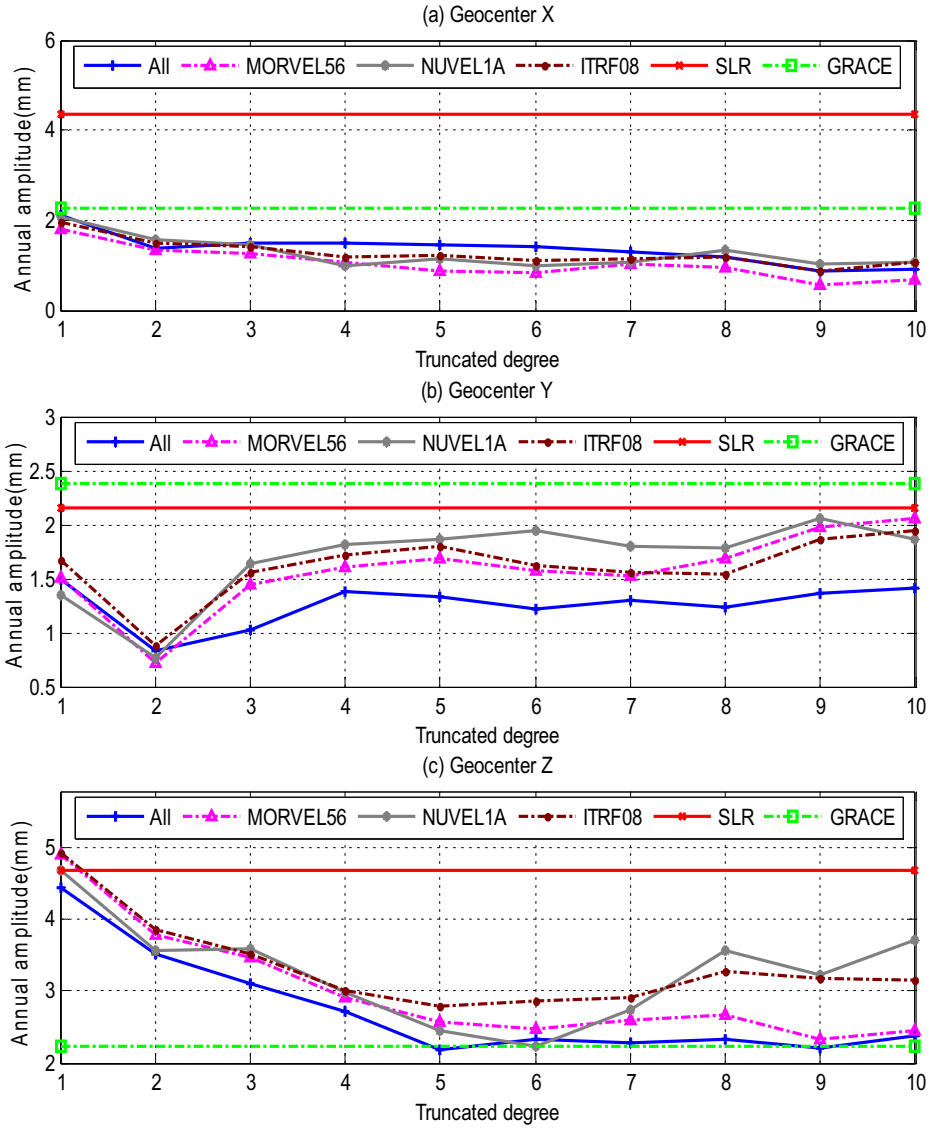

Fig. 8. Annual amplitudes of geocenter estimations from GPS observations with truncated degrees from 1 to 10. The symbols meanings are same as Fig. 2. (For interpretation of the references to color in this figure legend, the reader is referred to the web version of this article.)

well between different solutions. Semi-annual signal from GRACE is more significant in all three components. *MORVEL56 and ITRF08* and SLR also have semi-annual signals, except *NUVEL1A* and *All* in *X*, possibly because *NUVEL1A* have less used GPS stations and solutions from *All* are contaminated by deformed sites.

The amplitude and phase of the annual and semi-annual signals are determined with the following equation using unweighted least-square method:

$$y(t) = a + b(t - t_0) + \sum_{k=1}^{2}[A_k \cos(2\pi(t - t_0)/p_k - \phi_k)] \qquad (8)$$

where A_k is the amplitude, p_k is the period, ϕ_k is the phase in degree, t_{avg} is average time, t_0 is 1 January, a is constant and b is the trend. Tables 1 and 2 show annual and semi-annual amplitudes and phases. "All" means that all GPS sites are used without removing the deformed GPS sites, "MORVEL56" means that the selected rigid GPS sites are based on the MOREVEL56 plate motion model, "NUVEL1A" shows that the selected rigid GPS sites are based on the NUVEL1A plate motion model and "ITRF08" means that the selected rigid GPS sites are based on the ITRF08 plate motion model. Both annual amplitudes and phases are consistent well between GPS estimates, but large discrepancies of annual amplitudes are found between GPS and SLR. Annual amplitudes of geocenter motion from GPS are averagely 2.98, 0.8 and 1.12 mm, less than those from SLR in *X*, *Y* and *Z*, respectively, but closer to GRACE solutions. While annual phases from GPS are almost closer to SLR and GRACE. Semi-annual amplitudes of GPS results are closer to

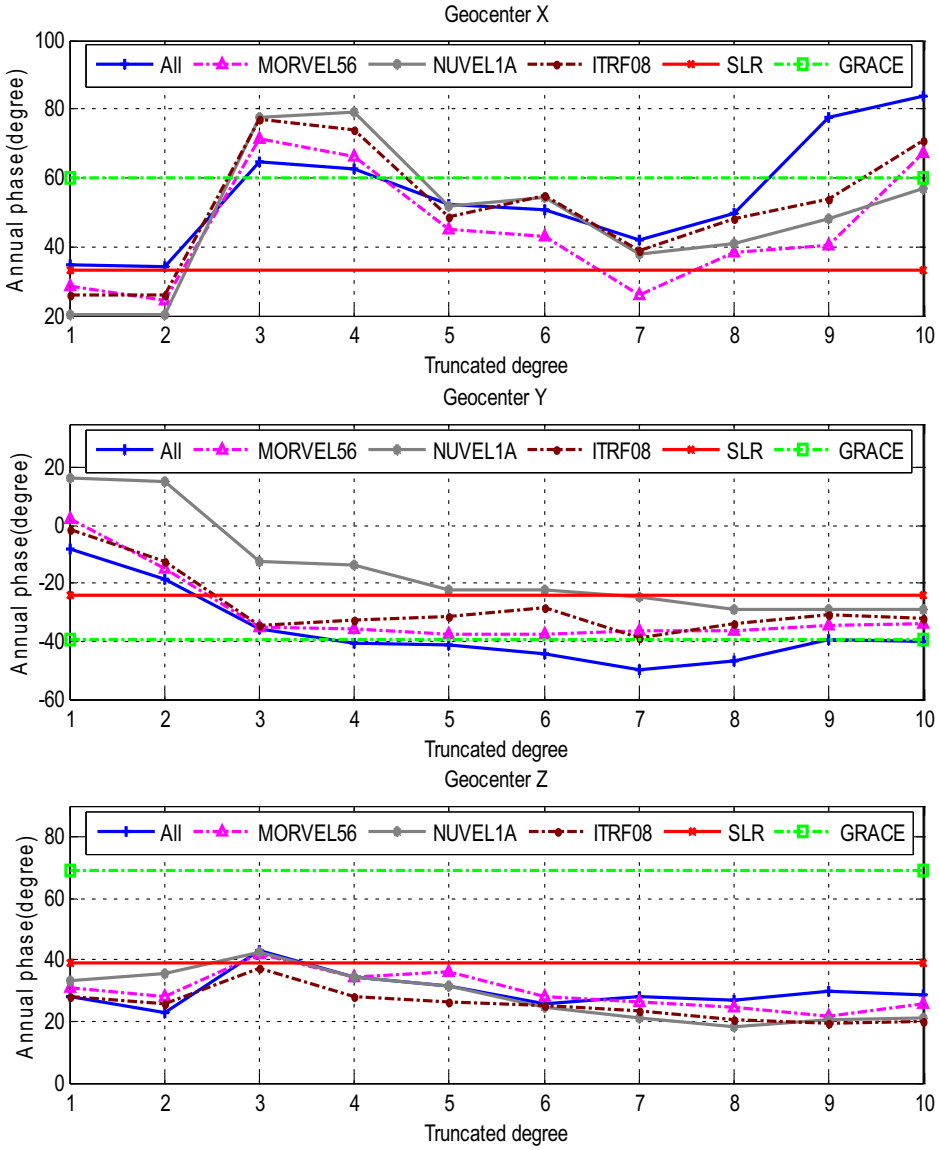

Fig. 9. Annual phases of geocenter estimations from GPS observations with truncated degrees from 1 to 10. The symbols meanings are same as Fig. 2. (For interpretation of the references to color in this figure legend, the reader is referred to the web version of this article.)

GRACE with less than 1 mm and semi-annual phases have large differences between different estimates although they agree well in X and Z for GPS and SLR.

5.2. Effects of truncated degrees and GPS network

5.2.1. RMS of geocenter estimates

RMS of residuals for each GPS strategy are less with truncated degree 3, averagely 1.2 mm in X and 1.4 mm in Y, 1.6 mm in Z, which are reduced by 23%, 14% and 17% in X, Y and Z respectively with respect to those with truncate degree 1. RMSs increase gradually after truncated degree 4, but are not larger than 2.3 mm (Fig. 7). The RMS w.r.t. GRACE has a minimum value with truncated degree 3 for each GPS estimate and *NUVEL1A* is the largest in Y (Fig. 4). The minimum of RMS of residuals and RMS w.r.t. GRACE are both located with truncated degree 3. With increase of truncated degrees, the aliasing errors have no big effect on the RMS, since the high degree coefficients are much smaller when compared to low degree coefficients.

5.2.2. Annual variations

Figs. 8 and 9 show the annual amplitudes and phases for different GPS strategies with truncated degrees from 1 to 10. The amplitudes and phases of SLR (red line) and GRACE (green line) are plotted horizontally. All GPS annual amplitudes vary greatly with smaller truncated degrees and become stable after truncated degree 3 in X, Y and Z, respectively. Annual amplitudes of GPS geocenter estimates in X are almost the same as each other, nearly equal to GRACE and half as big as that of SLR with all

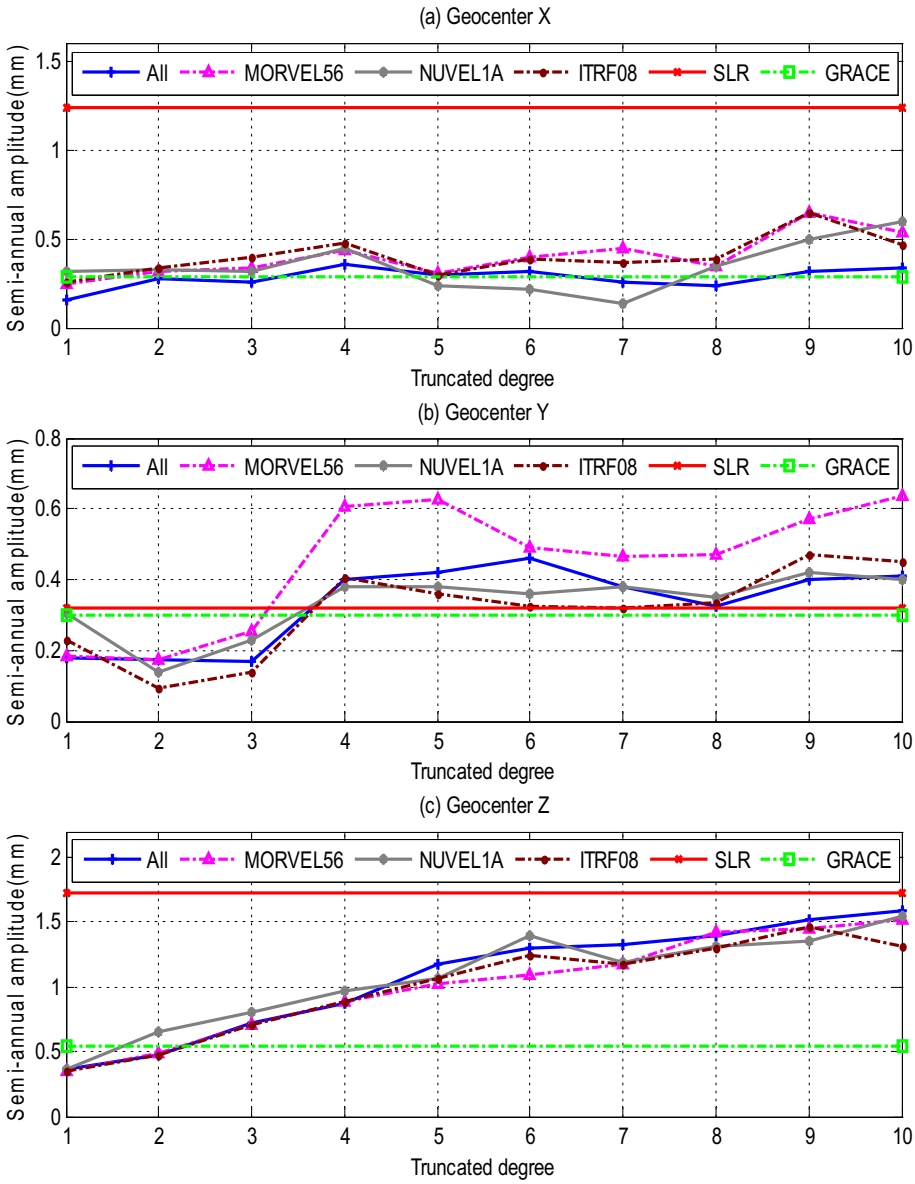

Fig. 10. Semi-annual amplitudes of geocenter estimations from GPS observations with truncated degrees from 1 to 10. The symbols meanings are same as Fig. 2.

truncated degrees, dropping about by 50% with truncated degree 2. Annual amplitudes of GPS, GRACE and SLR geocenter motions in Y are close except with truncated degree 2. Annual amplitudes of GPS in Z are closer to SLR with truncated degree 1, then decrease gradually and reach GRACE with truncated degree 5.

Annual phases of all GPS solutions in X are between 20° and 85°. Annual phases of all GPS solutions in Y decrease sharply from truncated degree 1 to 3 and then have a little variation with truncated degrees from 4 to 10. Furthermore, the patterns of *MORVEL56, ITRF08 and All* are very consistent and almost close to GRACE with truncated degrees from 3 to 10. However, the values of *NUVEL1A* are larger by about 20°. Annual phases of all GPS inversion in Z, about 40° less than GRACE and 10° less than SLR, are always stable except with truncated degree 3.

5.2.3. Semi-annual variations

Semi-annual amplitudes are presented in Fig. 10. GPS semi-annual amplitudes are stable with less than 0.5 mm and agree well with GRACE in X direction, vary between about 0.1 and 0.6 mm in Y direction, and gradually increase from about 0.25–1.5 mm in Z direction. The curves of all GPS semi-annual amplitudes agree well with each other except that *MORVEL56* has deviation with about 0.2 mm in Y direction from others.

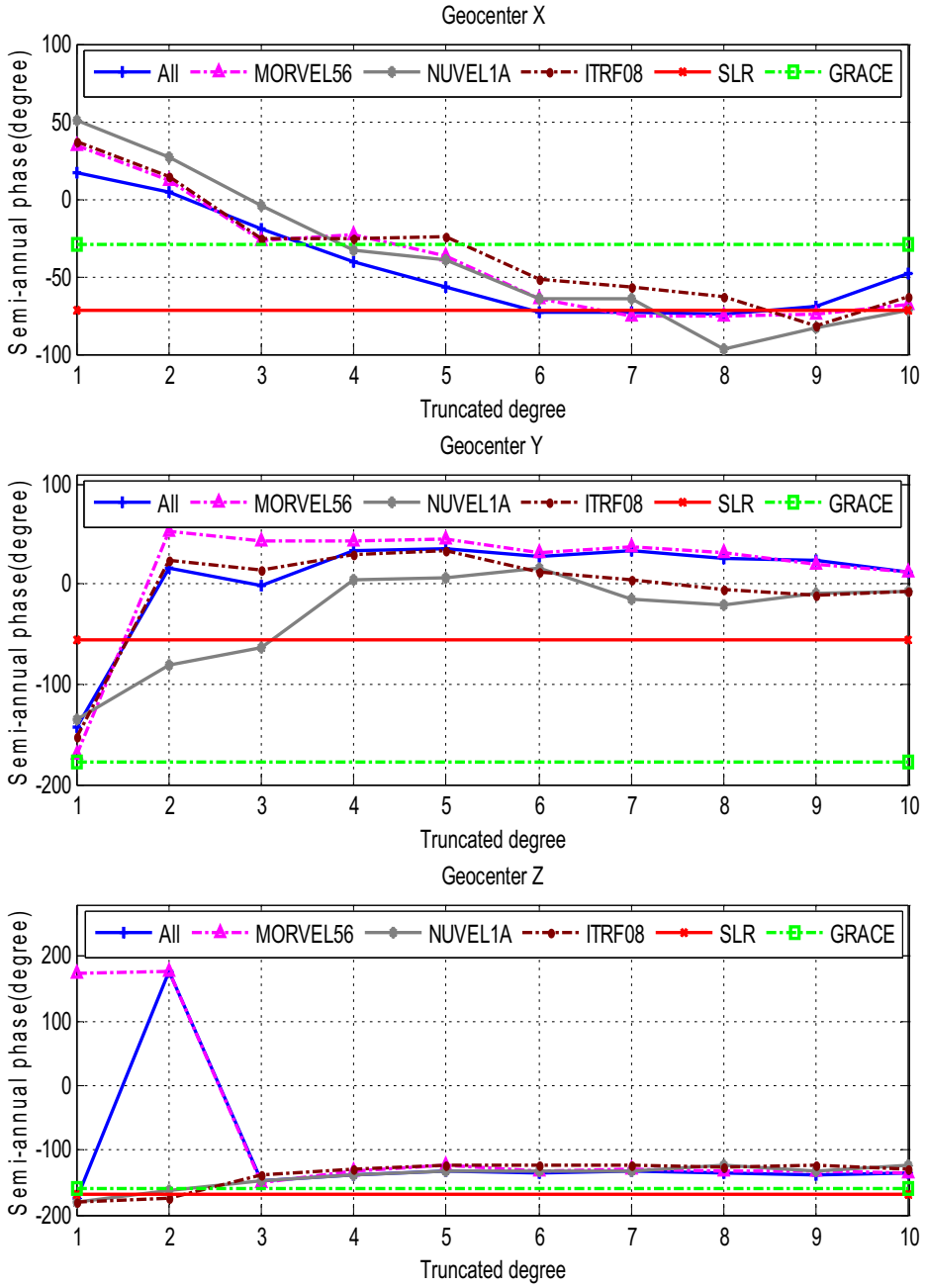

Fig. 11. Semi-annual phases of geocenter estimations from GPS observations with truncated degrees from 1 to 10. The symbols meanings are same as Fig. 2.

GPS semi-annual phases (Fig. 11) show the same way as annual phases. But semi-annual phases of GPS, GRACE and SLR geocenter motion do not match each other in Y component. Phases of GPS results almost linearly decrease between $-100°$ and $50°$ in X direction and suddenly jumps with truncated degree 2 and degree 3 in Z direction and then agrees with both SLR and GRACE after truncated degree 3.

6. Conclusion

Four sets of selected GPS networks are used to estimate geocenter motion according to loading theory, one is using all global GPS sites and the other three are selected by three plate motion models with removing sites whose velocity residuals are greater than 5.1 mm (3σ). Correlations of GPS geocenter motion estimates with GRACE in three components are much better than with SLR, especially in Y direction. The best correlations are estimates from GPS with truncated degree 3. RMSs of residuals and RMSs w.r.t. GRACE and SLR also support this conclusion. RMS of *NUVEL1A* in Y component is much higher than GPS estimates. Furthermore, geocenter estimates from GPS based on *MORVEL56* and *ITRF08* are better than NUVEL1A, while estimates from all GPS sites (*All*) are very similar to the *MORVEL56*, *GRACE* and *ITRF08*, which indicates that GPS sites selections have a little effect on geocenter estimates.

Annual geocenter amplitudes from GPS estimates are highly suffering from the aliasing errors of higher degrees, particularly in X and Z directions. The truncated degree 3 can reduce annual amplitudes by 29.2% in X, 5.6% in Y, 27.9% in Z w.r.t. the truncated degree 1. Annual amplitudes of all GPS estimates are almost the same as each other and closer to the GRACE than SLR in X, but smaller in Y. Annual phases of all GPS solutions from *MORVEL56, ITRF08* and *All* are very consistent and almost closer to GRACE solutions with truncated degrees from 3 to 10. However, the *NUVEL1A* is a little worse. Annual phases of all GPS estimates in Z are always stable except solutions with truncated degree 3. While the semi-annual signals are relatively weaker for all cases.

Therefore, the performance of GPS geocenter motion estimates depends on sites choices, but mostly the truncated degree. Currently more than 300 GPS sites are available, while 70% of the whole Earth (ocean areas) still has no or less GPS observations, In the future, it needs to further assess uncertainty and effects on geocenter estimates using more GPS observations.

Acknowledgments

We gratefully acknowledge the SOPAC to provide the processed GPS time series. This work was supported by the Main Direction Project of Chinese Academy of Sciences (Grant No. KJCX2- EW-T03), Shanghai Science and Technology Commission Project (Grant No. 12DZ2273300) and National Natural Science Foundation of China (NSFC) Project (Grant Nos. 11173050 and 11373059).

References

Altamimi, Z., Métivier, L., Collilieux, X., 2012. ITRF2008 plate motion model. J. Geophys. Res. 117, B07402. http://dx.doi.org/10.1029/2011JB008930.

Blewitt, G., 2003. Self-consistency in reference frames, geocenter definition, and surface loading of the solid Earth. J. Geophys. Res. 108 (B2), 2103.

Blewitt, G., Clarke, P., 2003. Inversion of Earth's changing shape to weigh sea level in static equilibrium with surface mass redistribution. J. Geophys. Res. 108 (B6), 2311.

Blewitt, G., Lavallée, D., Clarke, P., Nurutdinov, K., 2001. A new global mode of Earth deformation: seasonal cycle detected. Science 294 (5550), 2342–2345.

Cheng, M.K., Ries, J.C., Tapley, B.D., 2013. Geocenter variations from analysis of SLR data. Reference Frames for Applications in Geosciences, International Association of Geodesy Symposia, vol. 138. Springer-Verlag, Berlin Heidelberg, pp. 19–26.

DeMets, C., Gordon, R.G., Argus, D.F., Stein, S., 1994. Effect of recent revisions to the geomagnetic reversal time scale on estimates of current plate motions. Geophys. Res. Lett. 21 (20), 2191–2194.

DeMets, C., Gordon, R.G., Argus, D.F., 2010. Geologically current plate motions. Geophys. J. Int. 181 (1), 1–80.

Dong, D., Yunck, T., Heflin, M., 2003. Origin of the international terrestrial reference frame. J. Geophys. Res.: Solid Earth (1978–2012) 108 (B4), 1–8. http://dx.doi.org/10.1029/2002JB002035.

Farrell, W.E., 1972. Deformation of the Earth by surface loads. Rev. Geophys. 10 (3), 761–797.

Jin, S.G., Zhu, W.Y., 2004. A revision of the parameters of the NNR-NUVEL1A plate velocity model. J. Geodyn. 38 (1), 85–92. http://dx.doi.org/10.1016/j.jog.2004.03.004.

Jin, S.G., Chambers, D.P., Tapley, B.D., 2010. Hydrological and oceanic effects on polar motion from GRACE and models. J. Geophys. Res. 115, B02403. http://dx.doi.org/10.1029/2009JB006635.

Jin, S.G., Zhang, L., Tapley, B.D., 2011. The understanding of length-of-day variations from satellite gravity and laser ranging measurements. Geophys. J. Int. 184 (2), 651–660. http://dx.doi.org/10.1111/j.1365-246X.2010.04869.x.

Jin, S.G., Hassan, A.A., Feng, G.P., 2012. Assessment of terrestrial water contributions to polar motion from GRACE and hydrological models. J. Geodyn. 62, 40–48. http://dx.doi.org/10.1016/j.jog.2012.01.009.

Jin, S.G., van Dam, T., Wdowinski, S., 2013. Observing and understanding the Earth system variations from space geodesy. J. Geodyn. 72, 1–10. http://dx.doi.org/10.1016/j.jog.2013.08.001.

Lavallee, D.A., van Dam, T., Blewitt, G., Clarke, P.J., 2006. Geocenter motions from GPS: a unified observation model. J. Geophys. Res. 111, B05405. http://dx.doi.org/10.1029/2005JB003784.

Swenson, S., Chambers, D., Wahr, J., 2008. Estimating geocenter variations from a combination of GRACE and ocean model output. J. Geophys. Res.: Solid Earth (1978–2012) 113 (B8), 3.

Tregoning, P., van Dam, T., 2005. Effects of atmospheric pressure loading and seven-parameter transformations on estimates of geocenter motion and station heights from space geodetic observations. J. Geophys. Res. 110 (B3), B03408.

Wahr, J., Molenaar, M., Bryan, F., 1998. Time variability of the Earth's gravity field: Hydrological and oceanic effects and their possible detection using GRACE. J. Geophys. Res. 103 (B12), 30205–30230.

Wu, X., Argus, D.F., Heflin, M.B., Ivins, E.R., Webb, F.H., 2002. Site distribution and aliasing effects in the inversion for load coefficients and geocenter motion from GPS data. Geophys. Res. Lett. 29 (24), 63-1.

Wu, X., Ray, J., van Dam, T., 2012. Geocenter motion and its geodetic and geophysical implications. J. Geodyn. 58, 44–61.